

Real-time 3D analysis during electron tomography using tomviz

Received: 28 November 2021

Accepted: 15 July 2022

Published online: 01 August 2022

 Check for updates

Jonathan Schwartz¹, Chris Harris², Jacob Pietryga¹, Huihuo Zheng³, Prashant Kumar⁴, Anastasiia Visheratina⁴, Nicholas A. Kotov⁴, Brianna Major², Patrick Avery², Peter Ercius⁵, Utkarsh Ayachit², Berk Geveci², David A. Muller⁶, Alessandro Genova², Yi Jiang⁷, Marcus Hanwell^{2,8} & Robert Hovden^{1,9} ✉

The demand for high-throughput electron tomography is rapidly increasing in biological and material sciences. However, this 3D imaging technique is computationally bottlenecked by alignment and reconstruction which runs from hours to days. We demonstrate real-time tomography with dynamic 3D tomographic visualization to enable rapid interpretation of specimen structure immediately as data is collected on an electron microscope. Using geometrically complex chiral nanoparticles, we show volumetric interpretation can begin in less than 10 minutes and a high-quality tomogram is available within 30 minutes. Real-time tomography is integrated into tomviz, an open-source and cross-platform 3D data analysis tool that contains intuitive graphical user interfaces (GUI), to enable any scientist to characterize biological and material structure in 3D.

Three-dimensional (3D) characterization across the nanoscale is now possible using scanning/transmission electron microscopes (S/TEM)^{1–5}. In an electron tomography experiment, the volumetric structure of biological or material specimens is reconstructed from high-resolution projection images acquired across many viewing angles^{6,7}. Unfortunately, tomographic reconstructions can take one to several days to complete depending upon the dataset size or algorithm(s) employed. Even worse, the reconstruction occurs offline, long after all the data has been collected, preventing immediate interpretation during an ongoing experiment. While advancements in detector hardware have boosted throughput with digital data collection⁸, substantial human effort and computational resources are still required to process the raw data before visualization. It has been a longstanding goal to begin 3D analysis of specimens in real time to allow immediate assessment of nanoscale structure and data quality⁹.

Here we present facile 3D visualization of specimens during an electron or cryo-electron tomography experiment using the tomviz

platform (tomviz.org). Our platform now provides interactive 3D material or biological structure in real-time to enhance high-throughput specimen interpretation. Tomviz offers multiple real-time reconstruction algorithms integrated into a fully graphical interface that presents the user with immediate visualization during data collection. Achieving high-throughput electron tomography requires an integrated pipeline that links the microscope hardware to optimized reconstruction algorithms and efficient 3D volumetric visualization. A multi-threaded data analysis pipeline runs dynamic visualizations that update as new data is collected or reconstruction algorithms proceed. Iterative reconstruction algorithms efficiently accommodate new data and keep pace with typical experimental acquisition rates. Scientists can interactively analyze 3D specimen structure concurrent with a tomographic reconstruction after or during an experiment. The robust graphical interface allows for 3D specimens to be rendered as shaded contours or translucent volumes that can be rotated, cropped, or sliced

¹Department of Material Science and Engineering, University of Michigan, Ann Arbor, MI, USA. ²Kitware Inc, Clifton Park, NY, USA. ³Argonne Leadership Computing Facility, Argonne National Laboratory, Lemont, IL, USA. ⁴Department of Chemical Engineering, University of Michigan, Ann Arbor, MI, USA. ⁵The Molecular Foundry, Lawrence Berkeley National Laboratory, Berkeley, CA, USA. ⁶School of Applied and Engineering Physics, Cornell University, Ithaca, NY, USA. ⁷Advanced Photon Source, Argonne National Laboratory, Lemont, IL, USA. ⁸National Synchrotron Light Source II, Brookhaven National Laboratory, Upton, NY, USA. ⁹Applied Physics Program, University of Michigan, Ann Arbor, MI, USA. ✉e-mail: hovden@umich.edu

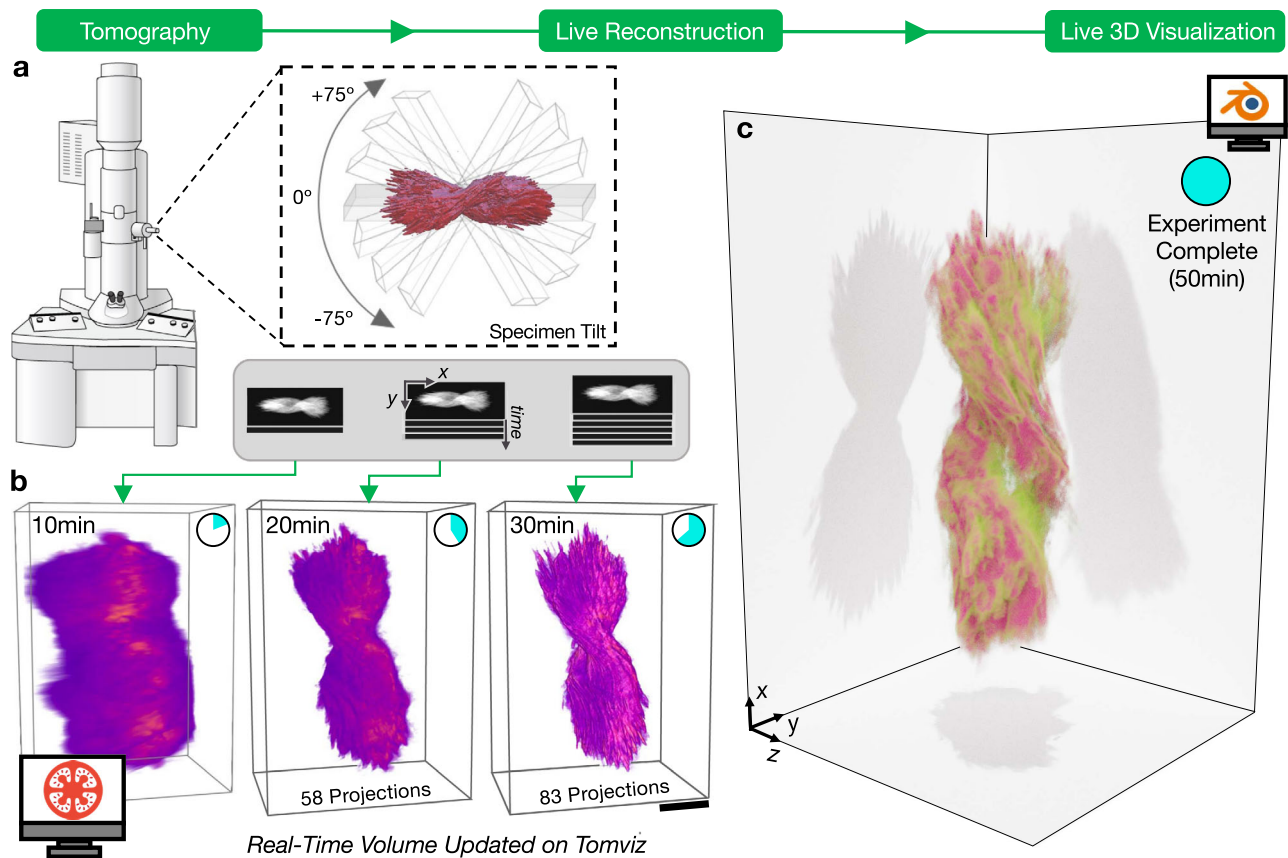


Fig. 1 | Real-time electron tomography workflow of a helical nanoparticle visualized on tomviz. **a** Specimen projections are sequentially collected in an electron microscope across an angular range ($\leq \pm 75^\circ$) and continually passed to tomviz for reconstruction and live 3D visualization. **b** As projections accumulate

during the experiment, the reconstruction updates in real-time and resolution improves. Scale bar, 100 nm **c** A high-quality tomogram is available for data interpretation upon the end of an experiment.

as the reconstruction occurs. In favorable cases, structural interpretation can begin as early as 10 min and a high-resolution volume is available after only 60% of data is acquired (~30 min). The latest tomviz release (v 2.0) is now packaged with real-time 3D analysis for electron tomography and is available as an open-source cross-platform tool with compiled binaries certified for Linux, Mac, and Windows.

Results

Real-time tomography workflow

The real-time tomography workflow is illustrated in Fig. 1: electron micrographs are collected, passed to tomviz for reconstruction, and visualized as an interactive 3D rendering. This process runs simultaneously and continuously while the electron microscope is being operated. During experimental acquisition, tomviz monitors when new projections are collected (Fig. 1a) and appends new data into the reconstruction process. Importantly, tomograms are reconstructed in parallel with data acquisition. Real-time algorithms accommodate the arrival of new data without restarting the reconstruction process. Iterative reconstruction methods are made efficient for real-time processes by utilizing dynamic descent parameters (see “Methods”). Dynamic reconstructions maintain pace with typical experimental acquisitions (e.g., 512^3 – 1024^3 voxels) using a personal computer. The intermediate reconstructions are rendered in 3D and immediately presented to the scientist (Fig. 1b). Thus, the tomogram dynamically improves with time as both the reconstruction algorithm converges and additional specimen information arrives. High-quality 3D reconstructions are available before the end of the experiment (Fig. 1c).

Early insight into 3D structure

Direct visualization of a specimen's 3D structure enables immediate identification of morphological and internal information shortly after a tomography experiment begins. We demonstrate real-time tomography on a helical nanoparticle comprised of a chiral dipeptide Cystine amino acid coordinated with Cadmium (Cyst/Cd) (Supplementary Videos S1, S2, and S7). The bowtie-shaped particles were synthesized using a size-limited self-assembly process described by Yan et al.¹⁰. These semiconducting nanoparticles contain strong tunable chiroptical properties due to a twisted geometry¹⁰. As shown in Fig. 1b, the overall morphology for the Cd/Cyst nanoparticle can be observed as early as 10 min and fine details are visible after 20–30 min of the experiment (roughly half-completion). The specimen's right-handed chirality cannot be determined from a single projection image and requires 3D imaging (Fig. 1c). With real-time tomography the material's chirality and symmetry were identified within the first third of data acquisition (~15 min). This immediate feedback can save researchers days of effort as reconstructions are no longer processed offline. Moreover, real-time visualization allows quick adjustment and optimization of reconstruction parameters that can greatly influence the reconstruction quality. Ultimately, scientists can efficiently investigate 3D nanostructure during imaging to guide experiments and redefine scientific objectives while simultaneously operating the microscope.

Real-time 3D visualization during reconstruction

Currently, the best tomographic reconstructions are obtained from algorithms that are slow and iterative. In practice, electron tomography experiments are limited by a finite and restricted angular range

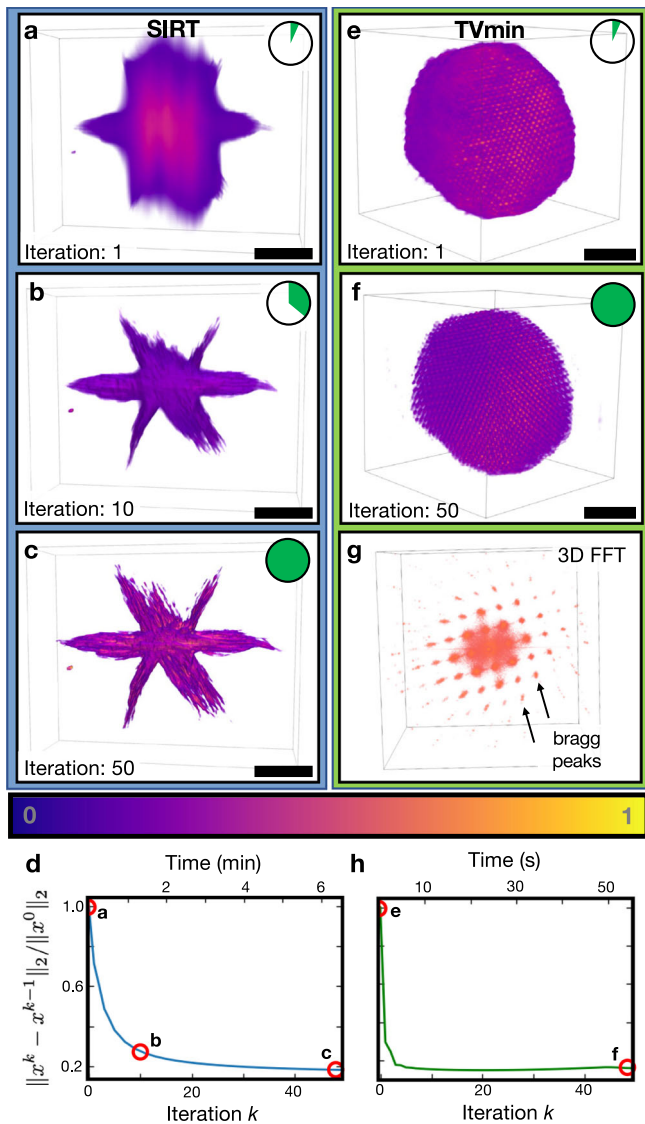


Fig. 2 | Demonstration of iterative reconstruction algorithms. **a–c** Visualization of the Co_2P nanoparticle early, mid, and at the end of the reconstruction process. At the beginning, the underlying structure can partially be seen behind the excess of background intensity. In the middle of the process, sharp features begin to form. The final iteration converges to a tomogram visually similar to the input tilt series. Scale bar, 50 nm. **e–g** Visualization of an atomic resolution FePt nanoparticle. The atoms in the TV nanoparticle are resolved with increasing iteration and its periodicity demonstrated with the fast Fourier transform (FFT). Scale bar, 1 nm. **d, h** A plot of the normalized residual to demonstrate convergence.

(e.g., $<\pm 70^\circ$) resulting in incomplete information that degrades resolution in 3D¹¹. Iterative algorithms can recover tomograms with high spatial resolution and minimal reconstruction error¹². While these algorithms better estimate 3D structure from under-determined measurements, they come at the expense of computational time¹³. Fortunately, using the tomviz tool, iterative reconstructions can be visualized in real-time throughout the arduous computation (Supplementary Videos S2 and S3).

Real-time tomography greatly alleviates the wait-time by visualizing the intermediate 3D structure between algorithm iterations—beneficial during an experiment or analysis. Figure 2 demonstrates interactive visualizations of the Simultaneous Iterative Reconstruction Technique (SIRT)¹⁴ for a cobalt phosphide (Co_2P) hyperbranched nanoparticle¹⁵ (512^3 voxels volume reconstructed across the 363.52 nm full field of view). SIRT tomograms begin with a loose estimate¹⁶

(Fig. 2a) and develop sharper, high-frequency information with each increasing iteration (Fig. 2b, c and Supplementary Video S4). Compressed sensing algorithms such as total variation minimization (TVmin) seek maximally sparse solutions to recover high-resolution, low-noise structures using fewer projections than conventional methods^{17,18}. Figure 2e, f and Supplementary Video S5 demonstrates an interactive 3D visualization using TVmin reconstruction of an iron platinum (FePt) nanoparticle at atomic resolution (256^3 voxels volume reconstructed across the 9.536 nm full field of view)—data provided and pre-processed by Yang et al.¹⁹. This work replicates the atomic resolution tomogram using independent pre-processing and reconstruction methods. Recent developments in dynamic compressive sensing²⁰ have also been incorporated into tomviz to accommodate the arrival of new projections during an experiment.

In addition to early estimates of specimen structure, real-time tomography allows assessment of the reconstruction convergence. This is observed qualitatively in the 3D visualization (Fig. 2e, f) and quantitatively plotted in the residuals (Fig. 2d, h). Watching the convergence provides visual inspection and intuition of how hyperparameters influence the final 3D structure and ensure proper convergence. For example, compressed-sensing-inspired reconstruction methods are sensitive to regularization weights and require visual inspection to assess accuracy²¹. Furthermore, these advanced reconstruction algorithms do not exhibit predictable or monotonic convergence a priori and require monitoring to optimize convergence and determine when to terminate^{22,23}. Even for traditional algorithms where convergence is more predictable, they are often slow and changes become marginal—the scientist need not wait to begin interpreting the 3D structure. Lastly, practical issues such as misalignment, spurious values in data (e.g., hot pixels), in-plane rotations, and other pre-processing artifacts alter or degrade a reconstruction; however, these problems are diagnosable without completing a full reconstruction. Real-time assessment saves researchers time by providing early feedback and optimizing reconstruction parameters to serve the long-standing goal of high-throughput tomography.

Alternatively, weighted back projection (WBP) reconstructions are ideal for quick assessment of specimen morphology due to their fast, non-iterative computation^{24,25}. Figure 3 shows screenshots taken from a live WBP reconstruction visualized using tomviz—time proceeds from left to right. Figure 3a is a tomogram of gold (Au) nanoparticles on strontium titanate (STO) nanocubes. Figure 3b shows platinum (Pt) nanoparticles on a carbon (C) support with the rotation axis along the x-direction. For WBP of single-axis tomography, partial volumetric updates are provided slice by slice along the direction parallel to the rotation axis. In the software, the 3D visualizations dynamically grow in one direction throughout the computation. Supplementary Video S6 shows the user experience of a WBP reconstruction emerging over just a few minutes.

The live tomography software

The latest tomviz release (v. 2.0) includes real-time tomography capabilities, is entirely open-source (BSD License), runs on all operating systems (OSX, Windows, Linux) with certified installers, and can be implemented on rudimentary TEMs available at most institutions. A user manual with step-by-step instructions for implementing real-time tomography is provided as a Supplementary Protocol along with Supplementary Video demonstrations (Supplementary Videos S3 and S4).

The tomviz graphical user interface (GUI) (Fig. 4) provides an intuitive tomography tool that allows scientists to focus on 3D specimen interpretation²⁶. Tomviz monitors data directories for the arrival of new projections during an experiment (Fig. 4a) and visualizes the 3D reconstruction as it dynamically updates (Fig. 4c). During a real-time tomographic reconstruction users can zoom, rotate, slice, and segment the object to highlight regions of interest as the algorithm runs independently. Each voxel in the 3D render (i.e., volumes or isometric

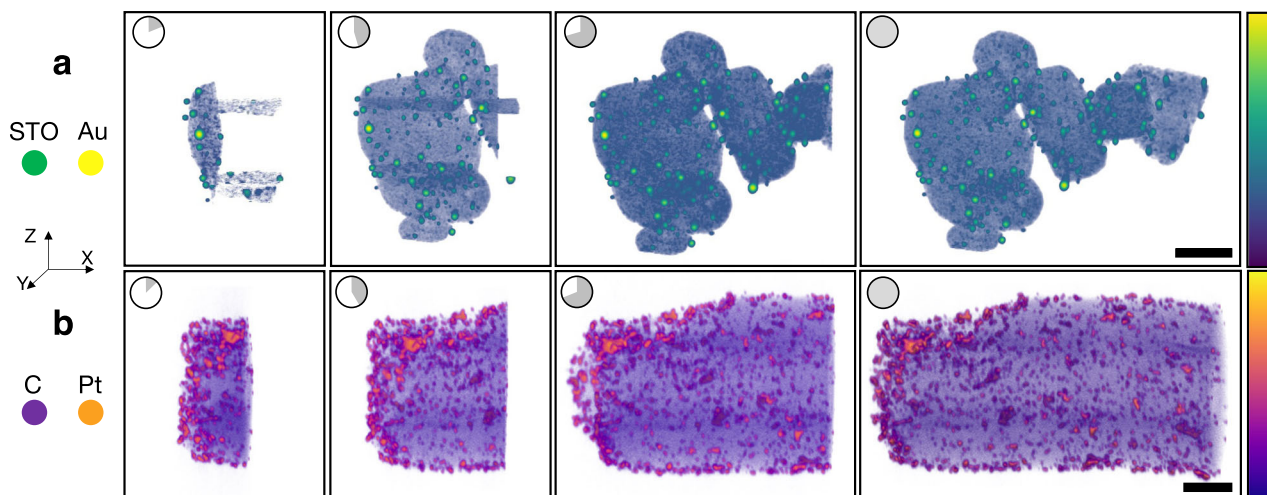


Fig. 3 | Demonstration of live WBP. Live tomographic reconstruction in tomviz shown through freeze frames during the progression of a weighted back-projection algorithm (left to right). This unique capability allows users to interact and analyze the 3D structure throughout reconstruction. In the actual software the

reconstruction updates in real time. **a** Live volume rendering of Au/strotrium titanate (STO) nanocubes. **b** Live volume rendering of platinum (Pt) nanoparticles on a carbon support. Scale bar, 50 nm.

contours) is assigned a color and opacity controlled by the color-opacity transfer function overlaid on the histogram visible at the top of the GUI (Fig. 4, top-right). Users can intuitively define voxel transparency by selecting points on the curve and dragging it between transparent and opaque. The data “Pipeline” retains all transformations and modules performed to produce visualizations, all of which can be saved in a state file for sharing and reproducibility.

A seamless user experience is enabled by an underlying multi-threaded framework of Python/C++ interactions. As the reconstruction occurs, algorithms written in Python trigger signals to notify the application that a new volume is available (“Methods”). Tomographic reconstructions can either run on basic computer infrastructure found on any laptop or scaled across multiple GPUs to process large volumes ($>1024^3$ voxels). Live reconstructions without performance degradation require a tripling of memory requirements. One data copy resides on the visualization (GUI) thread, another on the reconstruction (Python) thread, plus a temporary copy for efficient staging and handoff. The temporary copy allows the reconstruction to run unhindered during the handoff process. The total memory usage for real-time reconstruction is usually well within a consumer-grade computer (c.a. 0.4–16 GB). After the reconstruction is complete, all copies are released from memory and only the final reconstruction remains. Analytical reconstruction methods such as WBP can run slice-by-slice with new reconstructed slices appended along a single reconstruction direction. For iterative methods, we recommend updating the entire volume either every iteration or every few (depending on the speed of computation)—especially for complex sampling schemes such as dual or multiple-axis tomography that lacks a single rotation axes. Enhancements to the underlying 3D rendering (VTK) within tomviz were made to improve interactive visualization and analysis throughout the reconstruction process²⁷.

Discussion

We demonstrate real-time visualization of electron tomography reconstructions as they proceed during or after an experiment using tomviz, an open-source cross-platform tool compatible with all electron microscopes. We achieved real-time electron tomography by integrating dynamic volumetric data analysis tools, data input/output, processing, reconstruction, and visualization into a single software tool. In the actual software, the 3D visualizations are dynamically updated in parallel with computation. This means that scientists need not wait for reconstruction to complete, or all data to be collected

before beginning the interpretation of results. Continuous feedback provides high-throughput and early diagnoses of 3D specimens, opportunities to optimize experimental parameters, or investigate multiple regions of interest. Although dose is fundamentally set by the experimental acquisition parameters (e.g., dwell time, beam current, sampling rate, or tilt increment), in practice real-time tomography may reduce dose by streamlining acquisition and allowing the possibility of early termination if the reconstruction requirements are met. Optimized, threaded pipelines and the iterative nature of tomographic methods allow tomviz to show intermediate results with minimal impact on performance. This enables interactive 3D analysis of the current reconstruction state while the reconstruction proceeds on a separate thread. A robust graphical interface allows objects to be rendered as shaded contours or volumetric projections and these objects can be rotated, cropped, or sliced. This capability opens radically new possibilities for developing high-throughput, real-time tomographic reconstruction algorithms for geometrically complex inorganic²⁸ or biological materials. Ultimately, interactive real-time visualization goes beyond high-throughput and allows researchers to make early judgments to answer or identify new scientific questions during experimentation.

Methods

Installing tomviz

Tomviz binary installers are available at tomviz.org for macOS, Linux, or Windows²⁹. A user manual for real-time tomography using tomviz is provided as Supplemental Material.

Source-code availability

In addition to stable binary releases, the latest experimental builds and source code is available at github.com/OpenChemistry/tomviz. The entire package is built from 74,029 lines of code and 5253 merges to date³⁰. The application is primarily developed in C++ using CMake to coordinate the build process. Algorithms for electron tomography are primarily written using Python to offer facile in-app readability and modification. The entire code-base and dependencies are open-source and compiled to maximize reproducibility.

License

Tomviz and its underlying tomography algorithms are developed openly and freely as open source software under the 3-clause BSD License³¹—an Open Source Initiative approved license. This allows for

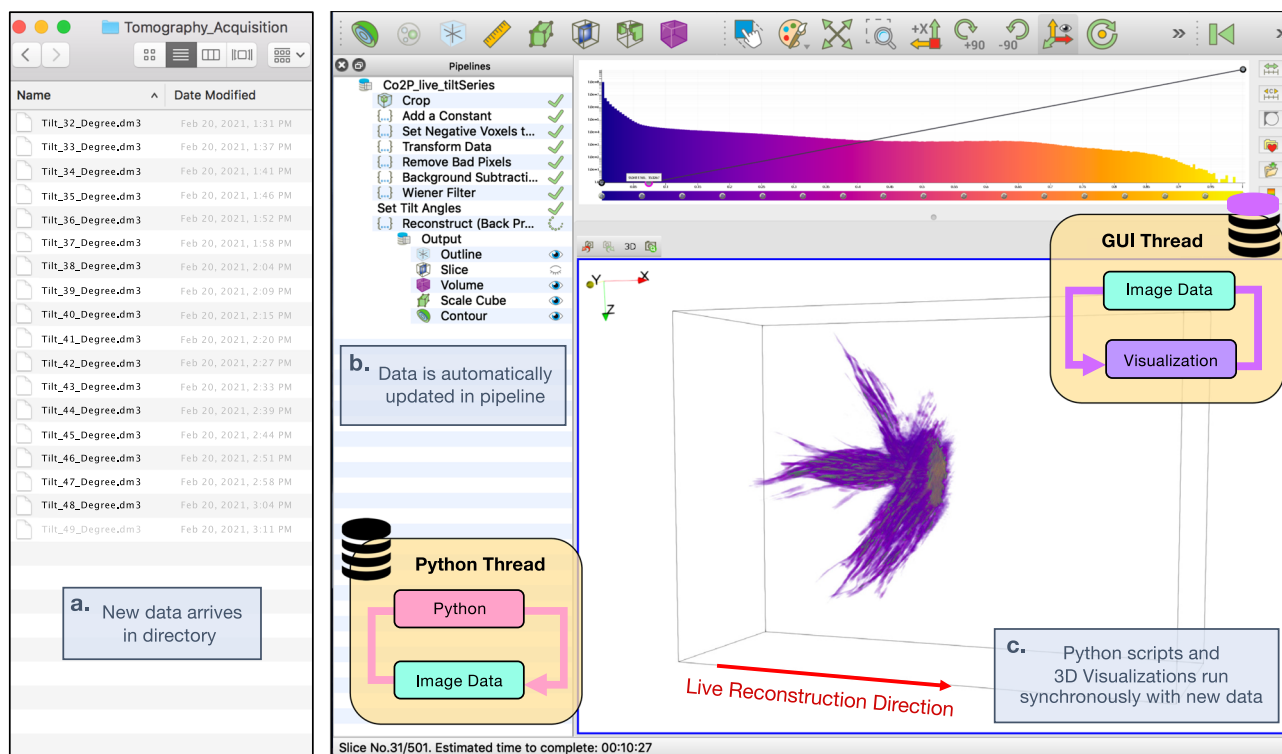


Fig. 4 | External and internal architecture of tomviz GUI. The tomviz platform is composed of a multi-threaded pipeline that synchronously handles tomographic and 3D visualization on separate threads. **a** Tomviz monitors for recently acquired

tilt projections within a directory and **b** automatically reads new data into the pipeline. **c** As tomographic reconstructions proceed, visualizations dynamically update and remain interactive for analysis.

unrestricted academic, commercial, and government use with no obligation on the part of the licensee to distribute the source code. This license encourages the widest possible re-use of the source code.

Specimen synthesis and preparation

Cyst/Cd helical nanoparticles are self-assembled via electrostatic and coordination interactions between positively charged cadmium ions and negatively charged chiral dipeptide cystine. The helical nanoparticles were mixed in an aqueous solution and drop cast using a micropipet onto a 3 mm copper TEM grid dried at room temperature. The TEM grid was an ultrathin (3 nm) carbon film with a large hexagonal mesh (100) to provide high specimen tilts without beam shadowing (Electron Microscopy Sciences, Hatfield, PA, USA). Specimen preparation for the Co₂P, C/Pt³², FePt¹⁹, and Au/STO³³ datasets are available in the cited manuscripts with data descriptors.

Electron tomography acquisition

Real-time electron tomography of the Cys/Cd helical nanoparticle (Fig. 1) was performed during experimental image acquisition on a Talos F200X (Thermo Fisher) operated at 200 kV with a 10.5 mrad semi-convergence angle using an annular dark field detector with an inner collection angle of 36 mrad. The projections were recorded from -64° to $+71^\circ$ with a $+1^\circ$ angular increment using a Model 2021 Fischione Analytical Tomography Holder. At each tilt angle, a STEM image with a $4 \mu\text{s}$ dwell time at each pixel of lateral dimension 2.47 nm. The tilt series for Figs. 2–4 were collected and aligned in advance of the real-time reconstruction. The FePt nanoparticle (Fig. 2f) was collected on a FEI Titan at 300 keV with a 30 mrad convergence angle and 1.5° tilt increment¹⁹. The Co₂P (Fig. 2c), Au/STO (Fig. 3a), and C/Pt (Fig. 3b)³² nanoparticles³³ were acquired on a FEI Tecnai F20 at 200 keV and 2° , 2° , and 1° tilt intervals, respectively. Additional experimental information is available in the corresponding references for each dataset.

A user manual with step-by-step instructions for implementing real-time tomography is provided as a Supplementary Protocol along with supplemental video demonstrations. As with any tomography experiment, microscope alignment is critical. In particular, the sample should be eucentric to alleviate specimen drift and the need for any stage refinement during acquisition. After the microscope is aligned, a user defines the data directory tomviz will monitor to bridge the pipeline from data acquisition to the 3D reconstruction and visualization. Because tomviz operates independently from the microscope acquisition control, this real-time tomography tool can run on any TEM and users can choose their preferred acquisition programs (e.g., Nion Swift³⁴, Digital Micrograph, FEI Velox, SerialEM³⁵).

File formats

Data stored as raw binaries, XDMF, HDF5, text, png, SER, DM3/4, or TIFF can be read into tomviz. This includes 32-bit IEEE floats. Users can save visualizations and computations as state files (.tvsm) to reproduce results and be shared among colleagues. Reconstructions can be exported into file formats compatible with dedicated 3D rendering software (e.g., Blender).

Data processing

Tomographic experiments require identification of the center of rotation in the projection tilt series; otherwise, artifacts will be introduced into the tomogram³⁶. Even after aligning the stage to eucentricity, the rotation axis can be offset from center and often require additional processing. When an object is tilted around the rotation axis, the object's center of mass (CoM) forms a circle and coincides with the origin of the perpendicular axis. To determine the CoM, we projected each projection onto the perpendicular axis and calculated its shift: $x_{CM} = \sum x_i \rho(x_i) / \sum \rho(x_i)$ where $\rho(x_i)$ is the Coulomb potential at position x_i ⁴. This method is known to be sensitive to noise, so prior to aligning the projections we performed a background subtraction to account for the sample support (lacey carbon) and increasing

thickness from high tilts. In our experiments, the uniform thin carbon support was removed by subtracting the average background scattered intensity.

Successful tilt axis identification with the center of mass alignment requires the total projected volume to be fixed for each projection³⁷ and objects to be isolated. In cases where either of these requirements are not met (e.g., slab specimen geometries or fields of view where multiple particles are visible), alternative alignment routines should be considered. We provide cross-correlation³⁸ for aligning non-isolated objects (Supplementary Fig. S3). For those that would like to perform marker-based alignment, we suggest using IMOD³⁹ prior to loading input projections in tomviz. Further tilt axis refinement can be selected with our automated identification script. More advanced iterative projection matching alignment routines can be utilized near the end of data collection to improve the tomogram resolution⁴⁰.

Real-time reconstruction algorithms during experimental acquisition

Modifications to the common implementation for SIRT and TVmin were made to account for the dynamic addition of input projections throughout an experiment. SIRT seeks the minimal error between the reconstruction and experimental data: $\arg \min_{\mathbf{x}} \|\mathbf{A}\mathbf{x} - \mathbf{b}\|_2$ where \mathbf{A} is the measurement matrix, \mathbf{b} is the experimental projections, and \mathbf{x} is the tomogram. We can further regularize the process through the assumption that our volumes should be piecewise smooth and minimize its total variation $\|\mathbf{x}\|_{TV}$. Iterative algorithms require rescaling of the descent parameter based on the number of projections sampled. SIRT can easily estimate the descent parameter through the calculation of the Lipschitz constant ($L = \|\mathbf{A}^T\mathbf{A}\|_2$). The Lipschitz constant can be estimated by using the power method⁴¹. The descent parameter for TVmin is scaled by a dampening envelope that ensures its magnitude decays linearly²⁰. Non-iterative algorithms such as WBP do not require rescaling of descent parameters and simply need to reinitialize the computation with the new projection images collected.

GUI parallelization for real-time visualization

The multithreaded pipeline within the tomviz application executes long-running jobs while simultaneously offering real-time visualization of the progress. As the reconstruction occurs, algorithms written in Python can trigger signals to notify the application that a new volume is available. A slot on the C++ side listens for this signal, using a mutually exclusive lock (mutex) on the image data to secure access to the updated volume. The new data is copied into the foreground thread (main GUI), and once it is available the mutex is released. Once the application receives a signal indicating that the output has been updated, downstream data operations can then be re-executed and any connected visualization modules will also be notified. As an effect, the histogram is recalculated in another background thread while all the current visualization modules display the rendered representation. In the case of the contour module, this will necessitate the recalculation of the surface mesh or the update will be uploaded to the GPU for volume rendering.

Data availability

Figure 1 and the user manual use exemplary data from Supplemental Dataset 1. The aligned and raw tilt series for the FePt dataset in Fig. 2 can be accessed through physics.ucla.edu/research/imaging/FePt. In addition, the projection images for the Co₂P and C-Pt nanoparticles displayed in Figs. 2 and 3 are available through doi.org/10.608432.

Code availability

Tomviz binaries are available as Supplementary Software and the source code can be downloaded from GitHub (github.com/OpenChemistry/tomviz).

References

1. Crowther, R., Amos, L., Finch, J., David, R. & Klug, A. Three dimensional reconstructions of spherical viruses by fourier synthesis from electron micrographs. *Nature* **226**, 421–425 (1970).
2. Medalia, O. et al. Macromolecular architecture in eukaryotic cells visualized by cryoelectron tomography. *Science* **298**, 1209–1213 (2002).
3. Midgley, P. & Weyland, M. 3d electron microscopy in the physical sciences: the development of z-contrast and eftem tomography. *Ultramicroscopy* **96**, 413–431 (2003).
4. Scott, M. et al. Electron tomography at 2.4-ångström resolution. *Nature* **483**, 444–447 (2012).
5. Yang, Y. et al. Determining the three-dimensional atomic structure of an amorphous solid. *Nature* **592**, 60–64 (2021).
6. David, R. & Klug, A. A reconstruction of three dimensional structures from electron micrographs. *Nature* **217**, 130–134 (1968).
7. Hoppe, W. & Hegerl, R. in *Computer Processing of Electron Microscope Images* 127–185 (Springer, 1980).
8. Schorb, M., Haberbosch, I., Wim, H., Schwab, Y. & Mastronarde, D. Software tools for automated transmission electron microscopy. *Nat. Methods* **16**, 471–477 (2019).
9. Burlage, J.-W. et al. Real-time reconstruction and visualization towards dynamic feedback control during time-resolved tomography experiments at tomcat. *Sci. Rep.* **9**, 18379 (2019).
10. Yan, J. et al. Self-assembly of chiral nanoparticles into semiconductor helices with tunable near-infrared optical activity. *Chem. Mater.* **32**, 476–488 (2019).
11. Orlova, E. & Saibil, H. Structural analysis of macromolecular assemblies by electron microscopy. *Chem. Rev.* **111**, 7710–7748 (2011).
12. Andersen, A. Algebraic reconstruction in CT from limited views. *IEEE Trans. Med. Imaging* **8**, 50–55 (1989).
13. Gazzola, S., Hansen, P. C. & Nagy, J. IR tools: a matlab package of iterative regularization methods and large-scale test problems. *Numer. Algor.* **81**, 773–811 (2018).
14. Gilbert, P. Iterative methods for the three-dimensional reconstruction of an object from projections. *J. Theor. Biol.* **36**, 105–117 (1972).
15. Zhang, H., Ha, D.-H., Hovden, R., Kourkoutis, L. & Robinson, R. Controlled synthesis of uniform cobalt phosphide hyperbranched nanocrystals using tri-n-octylphosphine oxide as a phosphorus source. *Nano Lett.* **11**, 189–197 (2010).
16. Xu, W. et al. High-performance iterative electron tomography reconstruction with long-object compensation using graphics processing units (GPUs). *J. Struct. Biol.* **171**, 142–153 (2010).
17. Sidky, E. & Pan, X. Image reconstruction in circular cone-beam computed tomography by constrained, total-variation minimization. *Phys. Med. Biol.* **53**, 4777–4807 (2018).
18. Sanders, T., Gelb, A., Platte, R., Arslan, I. & Landskron, K. Recovering fine details from under-resolved electron tomography data using higher order total variation l1 regularization. *Ultramicroscopy* **174**, 97–105 (2017).
19. Yang, Y. et al. Deciphering chemical order/disorder and material properties at the single-atom level. *Nature* **542**, 75–79 (2017).
20. Schwartz, J., Zheng, H., Hanwell, M., Jiang, Y. & Hovden, R. Dynamic compressed sensing for real-time tomographic reconstruction. *Ultramicroscopy* **219**, 113122 (2020).
21. Jiang, Y., Padgett, E., Hovden, R. & Muller, D. A. Sampling limits for electron tomography with sparsity-exploiting reconstructions. *Ultramicroscopy* **186**, 94–103 (2018).
22. Elfving, T., Hanser, P. C. & Touraj, N. Semi-convergence and relaxation parameters for a class of sirt algorithms. *Electron. Trans. Numer. Anal.* **37**, 321–336 (2010).
23. Elfving, T., Touraj, N. & Hanser, P. C. Semi-convergence properties of Kaczmarz's method. *Inverse Probl.* **30**, 055007 (2014).

24. Bracewell, R. Strip integration in radio astronomy. *Aust. J. Phys.* **9**, 198–217 (1956).
 25. Buurlage, J.-W., Bisseling, R. & Batenburg, J. A geometric partitioning method for distributed tomographic reconstruction. *Parallel Comput.* **81**, 104–121 (2019).
 26. Schwartz, J. et al. Real-time 3d analysis during tomographic experiments on tomviz. *Microsc. Microanal.* **27**(S1), 2860–2862 (2021).
 27. Hanwell, M. D., Martin, K. M., Chaudhary, A. & Avila, L. S. The visualization toolkit (vtk): Rewriting the rendering code for modern graphics cards. *SoftwareX* **1**, 9–12 (2015).
 28. Jiang, W. et al. Emergence of complexity in hierarchically organized chiral particles. *Science* 642–648 (2020).
 29. Levin, B. et al. Tutorial on the visualization of volumetric data using tomviz. *Microsc. Today* **26**, 12–17 (2018).
 30. Hanwell, M. et al. Tomviz. <https://github.com/OpenChemistry/tomviz/tree/1.10.0> (2021).
 31. Regents of the University of California. The BSD 3-Clause License. <http://opensource.org/licenses/BSD-3-Clause> (1990).
 32. Levin, B. et al. Nanomaterial datasets to advance tomography in scanning transmission electron microscopy. *Sci. Data* **3**, 160041 (2016).
 33. Padgett, E. et al. A simple preparation method for full-range electron tomography of nanoparticles and fine powders. *Microsc. Microanal.* **23**, 1150–1158 (2017).
 34. Meyer, C., Dellby, N., Lovejoy, T., Mittelberger, A. & Krivanek, O. Nion swift: open source image processing software for instrument control, data acquisition, organization, visualization, and analysis using python. *Microsc. Microanal.* **25**, 122–123 (2019).
 35. Mastronarde, D. Automated electron microscope tomography using robust prediction of specimen movements. *J. Struct. Biol.* **152**, 36–51 (2005).
 36. Donath, T., Beckmann, F. & Schreyer, A. Automated determination of the center of rotation in tomography data. *J. Opt. Soc. Am.* **23**, 1048–1057 (2006).
 37. Sanders, T., Prange, M., Akatay, C. & Binev, P. Physically motivated global alignment method for electron tomography. *Adv. Struct. Chem. Imaging* **1**, 4 (2015).
 38. Joachim, F. & McEwen, B. in *Alignment by Cross-Correlation* 205–213 (Springer US, 1992).
 39. Kremer, J. & Mastronarde, D. Computer visualization of three-dimensional image data using imod. *J. Struct. Biol.* **116**, 71–76 (1996).
 40. Odstrčil, M., Holler, M., Raabe, J. & Guizar-Sicairos, G. Alignment methods for nanotomography with deep subpixel accuracy. *Opt. Express* **27**, 36637–36652 (2019).
 41. Kazantsev, D. et al. Joint image reconstruction method with correlative multi-channel prior for x-ray spectral computed tomography. *Inverse Probl.* **34**, 064001 (2018).
- DE-AC02-06CH11357. P.E. is supported by the Molecular Foundry, Lawrence Berkeley National Laboratory, which is supported by the U.S. Department of Energy under contract no. DE-AC02-05CH11231. The authors thank Suk Hyun Sung and Yanqi Luo for input and feedback. Microscope illustration in Fig. 1 is released under creative commons license by Database Center for Life Science (DBCLS). This work made use of the Michigan Center for Materials Characterization (MC2) with technical support from Tao Ma and Bobby Kerns. The authors acknowledge financial support from the University of Michigan College of Engineering.

Author contributions

M.H. and R.H. conceived the idea. R.H., M.H., C.H., J.S., D.A.M., P.E., P.A., B.M., B.G., U.A., and A.G. designed tomviz's software and visualization architecture. J.S., J.P., Y.J., H.Z., and R.H. implemented real-time tomography algorithms. J.S., J.P., and R.H. conducted experiments. P.K., A.V., and N.A.K. synthesized Cyst/Cd nanoparticles. J.S. and R.H. wrote the manuscript. All authors reviewed and commented on the manuscript.

Competing interests

The authors declare no competing interests.

Additional information

Supplementary information The online version contains supplementary material available at <https://doi.org/10.1038/s41467-022-32046-0>.

Correspondence and requests for materials should be addressed to Robert Hovden.

Peer review information *Nature Communications* thanks the anonymous reviewers for their contribution to the peer review of this work. Peer reviewer reports are available.

Reprints and permission information is available at <http://www.nature.com/reprints>

Publisher's note Springer Nature remains neutral with regard to jurisdictional claims in published maps and institutional affiliations.

Open Access This article is licensed under a Creative Commons Attribution 4.0 International License, which permits use, sharing, adaptation, distribution and reproduction in any medium or format, as long as you give appropriate credit to the original author(s) and the source, provide a link to the Creative Commons license, and indicate if changes were made. The images or other third party material in this article are included in the article's Creative Commons license, unless indicated otherwise in a credit line to the material. If material is not included in the article's Creative Commons license and your intended use is not permitted by statutory regulation or exceeds the permitted use, you will need to obtain permission directly from the copyright holder. To view a copy of this license, visit <http://creativecommons.org/licenses/by/4.0/>.

© The Author(s) 2022

Acknowledgements

R.H. and J.S. acknowledge support from the Army Research Office, Computing Sciences (W911NF-17-S-0002). The tomviz project began with support under DOE Office of Science contract DE-SC0011385. This research used resources of the Argonne Leadership Computing Facility, which is a DOE Office of Science User Facility supported under Contract